

Polymer-Modified Opal Nanopores[†]

Olga Schepelina and Ilya Zharov*

Department of Chemistry, University of Utah, Salt Lake City, Utah 84112

Received April 28, 2006. In Final Form: July 14, 2006

The surface of nanopores in opal films, assembled from 205 nm silica spheres, was modified with poly(acrylamide) brushes using surface-initiated atom transfer radical polymerization. The colloidal crystal lattice remained unperturbed by the polymerization. The polymer brush thickness was controlled by polymerization time and was monitored by measuring the flux of redox species across the opal film using cyclic voltammetry. The nanopore size and polymer brush thickness were calculated on the basis of the limiting current change. Polymer brush thickness increased over the course of 26 h of polymerization in a logarithmic manner from 1.3 to 8.5 nm, leading to nanopores as small as 7.5 nm.

Introduction

Nanoporous membranes are attracting attention in fundamental research and technology^{1–3} because they enable control of molecule and ion transport on the nanoscale. To achieve such control, pores with suitable sizes have to be prepared, and their surfaces have to be chemically modified. Nanoporous membranes have been prepared using alumina,^{4,5} poly(ethylene terephthalate) and polyimide,^{6,7} and track-etched polycarbonate that can be further modified by wall-activated glow discharge⁸ or gold plating,⁹ polymers,¹⁰ zeolites,¹¹ silica,^{12,13} and nanotubes.^{14–16} Solid-state nanopores have been created in silicon oxide¹⁷ and silicon nitride^{18,19} and used to study DNA translocation.²⁰

Synthetic opals form via self-assembly of submicrometer-sized silica spheres into a close-packed face-centered cubic (fcc) lattice.²¹ The opals contain highly ordered arrays of 3D interconnected nanopores (Figure 1) whose size can be controlled by changing the size of the silica spheres used to assemble the opal (the distance from the center of the nanopore to the nearest

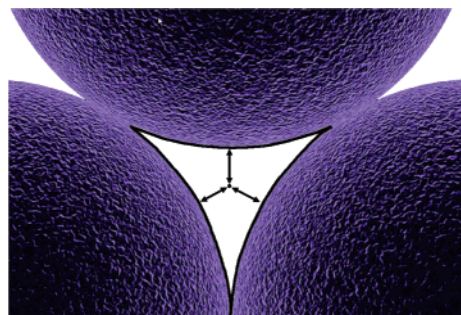


Figure 1. Schematic representation of an opal nanopore (traced with a black line). Distances from the pore center to the nearest sphere surface are shown with double-headed arrows.

silica sphere surface is ca. 15% of the sphere radius) and whose surface can be readily modified.²² The opal void fraction of 0.26 is independent of the size of the silica spheres, and the molecular flux normal to the (111) plane of an opal remains significant even when the opal pore size becomes sufficiently small to impart chemical selectivity.²³

Transport selectivity can be introduced into nanopores by modifying their surfaces with small organic molecules. For instance, the use of self-assembled monolayers on the surface of Au-plated nanotubes⁹ led to permselective nanoporous membranes.^{24–31} Charged silica surfaces have been shown to control the transport of ions through silica nanotubes.³² Recently, we showed that chemical selectivity can be introduced into

[†] Part of the Electrochemistry special issue.

(1) Tanev, P. T.; Butruille, J.-R.; Pinnavaia, T. J. In *Chemistry of Advanced Materials: An Overview*; Interrante, L. V., Hampden-Smith, M. J., Eds.; Wiley-VCH: New York, 1998; p 329.

(2) Davis, M. E. *Nature* **2002**, *417*, 813–821.

(3) Bayley, H.; Martin, C. R. *Chem. Rev.* **2000**, *100*, 2575–2594.

(4) Toh, C.-S.; Kayes, B. M.; Nemanick, E. J.; Lewis, N. S. *Nano Lett.* **2004**, *4*, 767–770.

(5) Yamaguchi, A.; Uejo, F.; Yoda, T.; Uchida, T.; Tanamura, Y.; Yamashita, T.; Teramae, N. *Nature Mater.* **2004**, *3*, 337–341.

(6) Siwy, Z.; Apel, P.; Baur, D. *Surf. Sci.* **2003**, *532*–535, 1061–1066.

(7) Siwy, Z. *Adv. Funct. Mater.* **2006**, *16*, 735–746.

(8) Ito, Y.; Park, Y. S.; Imanishi, Y. *J. Am. Chem. Soc.* **1997**, *119*, 2739–2740.

(9) Nishizawa, M.; Menon, V. P.; Martin, C. R. *Metal Science* **1995**, *268*, 700–702.

(10) Ulbricht, M. *Polymer* **2006**, *47*, 2217–2226.

(11) Kallus, S.; Condre, J.-M.; Hahn, A.; Golemme, G.; Algieri, C.; Dieudonne, P.; Timmins, P.; Ramsay, J. D. F. *J. Mater. Chem.* **2002**, *12*, 3343–3350.

(12) Nicole, L.; Boissiere, C.; Grosso, D.; Quach, A.; Sanchez, C. *J. Mater. Chem.* **2005**, *15*, 3598–3627.

(13) Liu, N. G.; Dunphy, D. R.; Atanassov, P.; Bunge, S. D.; Chen, Z.; Lopez, G. P.; Boyle, T. J.; Brinker, C. J. *Nano Lett.*, **2004**, *4*, 551–554.

(14) Hinds, B. J.; Chopra, N.; Rantell, T.; Andrews, R.; Gavalas, V.; Bachas, L. G. *Science* **2004**, *303*, 62–65.

(15) Miller, S. A.; Martin, C. R. *J. Am. Chem. Soc.* **2004**, *126*, 6226–6227.

(16) Sun, L.; Crooks, R. M. *J. Am. Chem. Soc.* **2002**, *122*, 12340–12345.

(17) Storm, A. J.; Chen, J. H.; Ling, X. S.; Zandbergen, H. W.; Dekker, C. *Nat. Mater.* **2003**, *2*, 537–540.

(18) Tong, H. D.; Jansen, H. V.; Gadgil, V. J.; Bostan, C. G.; Berenschot, C. G. E.; van Rijn, C. J. M.; Elwenspoek, M. *Nano Lett.* **2004**, *4*, 283–287.

(19) Heng, J. B.; Aksimentiev, A.; Ho, C.; Timp, G. *Biophys. J.* **2006**, *90*, 1098–1106.

(20) Storm, A.; Storm, C.; Dekker, C. *Nano Lett.* **2005**, *5*, 1193–1197.

(21) Wong, S.; Kitaev, V.; Ozin, G. A. *J. Am. Chem. Soc.* **2003**, *125*, 15589–15598.

(22) Ravoo, B. J.; Reinhoudt, D. N.; Onclin, S. *Angew. Chem., Int. Ed.* **2005**, *44*, 6282–6304.

(23) Newton, M. R.; Morey, K. A.; Zhang, Y.; Snow, R. J.; Diwekar, M.; Shi, J.; White, H. S. *Nano Lett.* **2004**, *4*, 875–880.

(24) Kohli, P.; Harrell, C. C.; Cao, Z.; Gasparac, R.; Tan, W.; Martin, C. R. *Science* **2004**, *305*, 984–986.

(25) Harrell, C. C.; Lee, S. B.; Martin, C. R. *Anal. Chem.* **2003**, *75*, 6861–6867.

(26) Chun, K.-Y.; Stroeve, P. *Langmuir* **2002**, *18*, 4653–4658.

(27) Ku, J.-R.; Stroeve, P. *Langmuir* **2004**, *20*, 2030–2032.

(28) Hulteen, J. C.; Jirage, K. B.; Martin, C. R. *J. Am. Chem. Soc.* **1998**, *120*, 6603–6604.

(29) Jirage, K. B.; Hulteen, J. C.; Martin, C. R. *Anal. Chem.* **1999**, *71*, 4913–4918.

(30) Siwy, Z.; Heins, E.; Harrell, C. C.; Kohli, P.; Martin, C. R. *J. Am. Chem. Soc.* **2004**, *126*, 10850–10851.

(31) Siwy, Z.; Trofin, L.; Kohli, P.; Baker, L. A.; Trautmann, C.; Martin, C. R. *J. Am. Chem. Soc.* **2005**, *127*, 5000–5001.

(32) Karnik, R.; Fan, R.; Yue, R.; Li, D.; Yang, P.; Majumdar, A. *Nano Lett.* **2005**, *5*, 943–948.

nanoporous opal films by surface modification with amines^{33,34} and chiral selector molecules.³⁵

Another approach to controlled transport through pores is to modify their surfaces with polymers. It has been demonstrated that transport selectivity could be built into micrometer- and submicrometer-sized pores using grafted macromolecules that respond to environmental stimuli,³⁶ including pH-responsive polypeptides,^{37,38} light-responsive spirobenzopyran-containing copolymers,³⁹ and ion-responsive polymers.⁴⁰ Au-plated nanotubes have been modified with biopolymers to provide chiral selectivity to the transport through such nanotubes.⁴¹

By placing polymer molecules inside opal nanopores, both their size and transport selectivity could be controlled. The success of such an approach depends on the ability to modify opal nanopore surfaces with macromolecules in a uniform and reproducible fashion without perturbing the colloidal crystal lattice. A natural choice for such a modification is a surface-initiated radical living polymerization that has been widely used to create uniform polymer brushes on flat surfaces.^{42–44} By utilizing living radical polymerizations, control over polymer molecular weight and brush thickness as well as relatively low polydispersity can be achieved. In particular, surface-initiated atom transfer radical polymerization (ATRP)⁴⁵ has been demonstrated to be a robust method for the preparation of well-defined polymer brushes.⁴⁶ In recent studies, the rapid growth of polymer brushes using a highly active ATRP catalyst has been described.⁴⁷

Surface-initiated polymerization from silica nanoparticles has been well studied.^{48,49} Recently, dense, homogeneous poly(methyl methacrylate) brushes were prepared on the surface of a glass filter with a wide distribution of pore sizes in the micrometer range by surface-initiated radical living polymerization.⁵⁰ Uniform poly(acrylamide) brushes were prepared by surface-initiated ATRP on silica.^{51,52}

In the present work, we describe the polymerization of acrylamide inside highly ordered nanopores in opal films assembled from 205 nm silica spheres and diffusion through the resulting polymer-modified nanopores. This is the first time that surface-initiated ATRP has been performed in a colloidal crystal and polymer brushes have been prepared inside its nanopores. Recently, photonic crystal films have been coated with layers

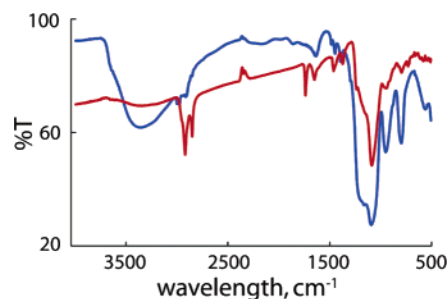


Figure 2. IR spectra of the unmodified silica spheres (blue) and silica spheres after polymer brush formation (red).

of polyelectrolytes.⁵³ We demonstrate that polymerization does not perturb the colloidal crystal and that opal nanopore sizes can be controlled by varying the polymerization time. Because the interior of a 3D opal nanopore is difficult to image directly, we use cyclic voltammetry, which provides a simple way of characterizing the geometry of nanopores in films deposited on an electrode surface (Figure 3).^{54,55}

Experimental Section

Materials and Reagents. Copper(I) chloride (anhydrous, 99.99%), bipyridine (99%), acrylamide (electrophoresis grade, 99.9%), and tetraethyl orthosilicate (99.99%) were obtained from Aldrich and used as received. 1-(Trichlorosilyl)-2-[*m/p*-(chloromethyl) phenyl] ethane was obtained from Gelest as a mixture of isomers. Hexaamineruthenium(III) chloride (99%, Strem Chemicals) and potassium chloride (99%, Mallinckrodt) were used as received. Toluene (Mallinckrodt) was distilled before use. Water (18 M Ω ·cm) was obtained from a Barnsted E-pure water purification system.

Preparation and Modification of Silica Spheres in Solution. A solution of tetraethoxysilane (TEOS) in absolute ethanol was rapidly poured into a stirred mixture of ammonia and water in absolute ethanol at room temperature. The final concentrations of the reagents were 0.2 M TEOS, 0.4 M ammonia, and 17 M water. After the reaction mixture was stirred for 18 h, the spheres were isolated by repeated centrifugation and resuspension in absolute ethanol. The diameter of the spheres was found to be 205 \pm 5 nm using scanning electron microscopy (SEM).

The functionalization of silica spheres suspended in toluene was achieved by treatment with a 1.5-fold excess of 1-(trichlorosilyl)-2-[*m/p*-(chloromethyl)phenyl]-ethane for 18 h at 70 °C. The particles were isolated via centrifugation and washed by four cycles of centrifugation and resuspension in toluene, MeOH, CH₂Cl₂, and acetone in order to remove any adsorbed initiator. To determine the surface coverage of the initiator-modified silica spheres, known concentration solutions of 1-(trichlorosilyl)-2-[*m/p*-(chloromethyl) phenyl]-ethane were prepared, and the extinction coefficient was determined to be $\epsilon = 2807 \text{ M}^{-1}$ at 242 nm. Next, UV spectra were obtained for colloidal solutions of silica spheres modified with initiator moieties (0.054 g in 10 mL of CHCl₃ for the initial measurement and subsequent dilution). The surface coverage was calculated on the basis of the absorbance at 242 nm and using a density of 2.07 g/cm³ for the silica spheres.

Initiator-modified silica spheres (799 mg) were placed into a three-necked flask containing CuCl (15 mg), bipyridine (70 mg), and acrylamide (1.67 g). DMF (12 mL) was purged with nitrogen for 1 h and added to the mixture, and the flask was degassed (four freeze/vacuum/N₂ cycles). The mixture was stirred and sonicated to obtain a uniform suspension. The mixture was then stirred at 90 °C. Periodically, samples were taken using a syringe. PAAm-silica nanoparticles were precipitated in methanol, washed with large

(33) Newton, M. R.; Bohaty, A. K.; White, H. S.; Zharov, I. *J. Am. Chem. Soc.* **2005**, *127*, 7268–7269.

(34) Newton, M. R.; Bohaty, A. K.; Zhang, Y.; White, H. S.; Zharov, I. *Langmuir* **2006**, *22*, 4429–4432.

(35) Cichelli, J.; Zharov, I. *J. Am. Chem. Soc.* **2006**, *128*, 8130–8131.

(36) Ito, Y.; Park, Y. S. *Polym. Adv. Technol.* **2000**, *11*, 136–144.

(37) Smuleac, V.; Butterfield, D. A.; Bhattacharyya, D. *Chem. Mater.* **2004**, *16*, 2762–2771.

(38) Ito, Y.; Park, Y. S.; Imahishi, Y. *Langmuir* **2000**, *16*, 5376–5381.

(39) Ito, Y.; Park, Y. S.; Imahishi, Y. *Macromolecules* **1998**, *31*, 2606–2610.

(40) Yamaguchi, T.; Ito, T. *J. Am. Chem. Soc.* **2004**, *126*, 6202–6203.

(41) Lee, S. B.; Mitchell, D. T.; Trofin, L.; Nevanen, T. K.; Söderlund, H.; Martin, C. R. *Science* **2002**, *296*, 2198–2201.

(42) Edmondson, S.; Osborne, V. L.; Huck, W. T. S. *Chem. Soc. Rev.* **2004**, *33*, 14–22.

(43) *Polymer Brushes: Synthesis, Characterization, Applications*. Advincula, R. C., Ed.; Wiley-VCH: Weinheim, Germany, 2004.

(44) Husseman, M.; Malmstrom, E. E.; McNamara, M.; Hedrick, J. L.; Russell, T. P.; Hawker, C. J. *Macromolecules* **1999**, *32*, 1424–1431.

(45) Wang, J.; Matyjaszewski, K. *Macromolecules* **1995**, *28*, 7901–7910.

(46) Pyun, J.; Kowalewski, T.; Matyjaszewski, K. *Macromol. Rapid Commun.* **2003**, *24*, 1043–1059.

(47) Bao, Z.; Bruening, M. L.; Baker, G. L. *J. Am. Chem. Soc.* **2006**, *128*, 9056–9060.

(48) Radhakrishnan, B.; Ranjan, R.; Brittain, W. J. *Soft Matter* **2006**, *2*, 386–396.

(49) Werne, T.; Patten, T. E. *J. Am. Chem. Soc.* **1999**, *121*, 7409–7410.

(50) Ejaz, M.; Tsujii, Y.; Fukuda, T. *Polymer* **2001**, *42*, 6811–6815.

(51) Huang, X.; Wirth, M. J. *Anal. Chem.* **1997**, *69*, 4577–4580.

(52) Xiau, D.; Wirth, M. J. *Macromolecules* **2002**, *35*, 2919–2925.

(53) Arsenaault, A. C.; Halfyard, J.; Wang, Z.; Kitaev, V.; Ozing, G. A.; Manners, I. *Langmuir* **2005**, *21*, 499–503.

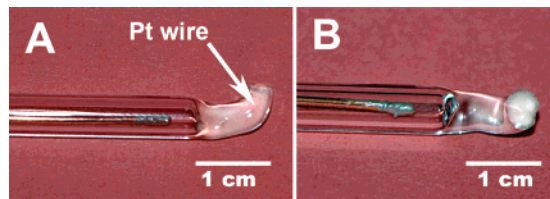
(54) Naegeli, R.; Redepenning, J.; Anson, F. C. *J. Phys. Chem.* **1986**, *90*, 6227–6232.

(55) Redepenning, J.; Anson, F. C. *J. Phys. Chem.* **1987**, *91*, 4549–4553.

Table 1. TGA Data^a for Polymer-Modified Silica Spheres at Different Polymerization Times

bare	initiator mod.	polymerization time, h			
		2	6	18	43
6	7	13	15	17	20

^a Percent weight loss at 800 °C.

**Figure 3.** (A) Side and (B) front view photographs of the opal film electrode.

amounts of MeOH, distilled water, and acetone, and dried. Infrared spectroscopy (Figure 2) and thermogravimetric analysis (Table 1) were used to characterize polymer-coated silica particles.

Pt Microdisk Electrodes. Pt microdisk electrodes (25 μm in diameter) shrouded in glass were prepared by first attaching a 1.0-mm-diameter Cu wire (Alfa Aesar) to a 25- μm -diameter Pt wire using Ag paint (Du Pont). The Pt wire was then flame sealed in a glass capillary; the capillary was bent into a U shape, and the middle was cut orthogonal to the length of the capillary with a diamond saw to expose the Pt disk. The resulting electrodes (Figure 3) were polished with Microcut Paper disks (Buehler), from 240 to 1200 grit in succession, until the surface was free from visible defects.

Preparation of Initiator-Modified Opal Films. Opal films were deposited on the electrode surfaces by placing the electrodes vertically in a 1.5 wt % colloidal solution of 205 nm silica spheres in ethanol and letting the solvent evaporate for 2 to 3 days in a vibration-free environment. The 1.5 wt % silica spheres solution produced 35-layer films with a thickness of ca. 7 μm as was determined by SEM.

The surface of the silica spheres assembled into opal films on the Pt electrodes was modified by immersing the electrodes under nitrogen in dry toluene containing 0.06 M 1-(trichlorosilyl)-2-[*m/p*-(chloromethyl) phenyl]-ethane. The reaction proceeded at 70 °C for 18 h. After modification, the electrodes were soaked and rinsed with dry toluene.

Surface-Initiated ATRP of Acrylamide on Opal Films. CuCl (45 mg), Bipy (0.21 g), acrylamide (5 g), and 10 mL of DMF (purged with nitrogen for 1 h) were placed in a three-necked round-bottomed flask, and the flask was degassed (four freeze/vacuum/ N_2 cycles). The electrode with an initiator-modified opal film was hung down vertically into the flask. The reaction mixture was stirred at 90 °C. The polymerization time was varied from 15 min to 43 h. After the reaction, the electrode was rinsed with DMF, acetonitrile, and water.

Characterization. The molecular flux across the opal film was measured voltammetrically using a Par model 175 universal programmer and a Dagan Cornerstone Chem-Clamp potentiostat. The voltammetric response of the bare, opal-, and polymer-modified

Table 2. Silica Sphere Diameter (d) and Polymer Brush Thickness (Δr) as Functions of Polymerization Time

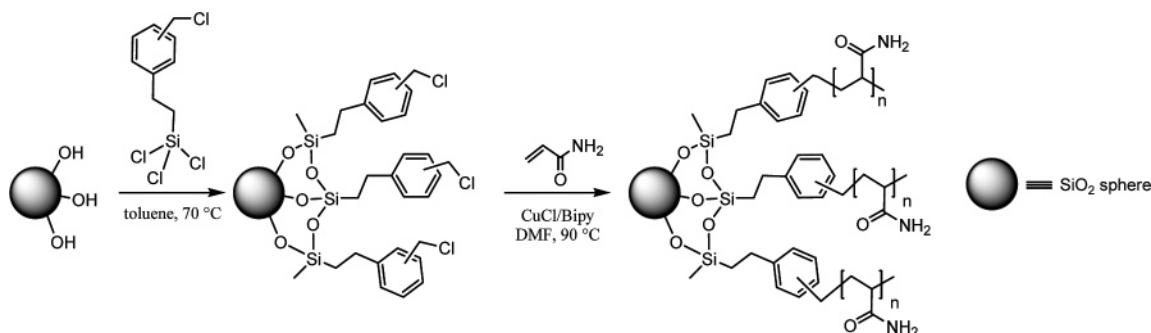
polymerization time, h	DLS		SEM	
	d , nm	Δr , nm	d , nm	Δr , nm
0	238 \pm 13	0	205 \pm 5	0
2	248 \pm 8	5.0	219 \pm 11	7.0
6	257 \pm 4	9.5	230 \pm 15	12.5
18	261 \pm 10	11.5	233 \pm 13	14.0
27	263 \pm 13	12.5	234 \pm 14	14.5
43	264 \pm 15	13.0	236 \pm 16	15.5

opal electrodes was measured in a 5.1 mM aqueous solution of $\text{Ru}(\text{NH}_3)_6^{3+}$ and 0.2 M KCl as the supporting electrolyte. Aqueous solutions were prepared using 18 $\text{M}\Omega\cdot\text{cm}$ water and purged with nitrogen to remove dissolved oxygen. Thermogravimetric analysis of polymer-coated silica particles was conducted using TGA Q500 (TA Instruments). Dynamic light scattering (Brookhaven ZetaPALS) and scanning electron microscopy (Hitachi S3000-N) were employed to perform size characterization of polymer-modified silica spheres. UV spectra were recorded using an Ocean Optics USB2000 instrument.

Results and Discussion

Surface Modification of Silica Spheres in Solution. An important advantage of using self-assembled opal films as nanoporous membranes is the ability to study the surface modification of the silica spheres in a colloidal solution, with the assumption that similar processes take place on silica sphere surfaces after their assembly into the opal. Thus, to model the polymerization that would take place inside the opal nanopores, we modified 205-nm-diameter silica spheres with initiator molecules in solution (Scheme 1). The number of initiator moieties, determined by UV spectroscopy, was ca. 4 molecules/ nm^2 , which corresponds to near-monolayer coverage⁵⁶ of the surface with initiator moieties. The resulting modified silica spheres were treated with acrylamide in the presence of copper(I) chloride and bipyridine to form the polymeric brush (Scheme 1). The formation of the polymer was confirmed by IR spectroscopy (Figure 2). The IR spectrum of the silica spheres after polymerization shows signals at 1700 and 3200, characteristic of amide groups, and at 2900 cm^{-1} , corresponding to alkyl C–H groups. Thermogravimetric analysis (TGA) at 800 °C (Table 1) revealed that with increasing polymerization time a thicker polymer brush is formed, as expected.

To monitor the thickness of the polymer brush on silica spheres in solution as a function of polymerization time, we measured the sphere diameters using dynamic light scattering (DLS) and scanning electron microscopy (SEM). The results of these measurements are shown in Table 2. The absolute diameter of the spheres determined by DLS is ca. 30 nm larger than that determined by SEM, which is likely the result of the polymer

Scheme 1

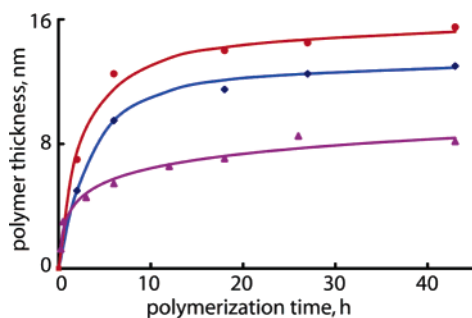


Figure 4. Polymer brush thickness as a function of polymerization time measured by SEM (red) and DLS (blue) for silica spheres in solution and calculated for opal nanopores using cyclic voltammetry results (purple).

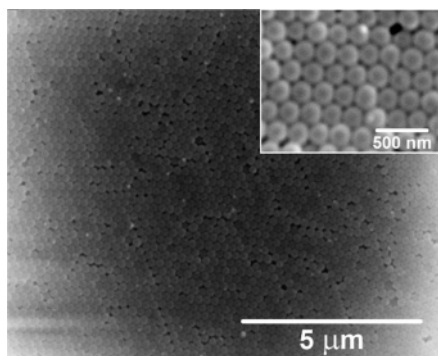


Figure 5. SEM image of the opal film assembled from 205 nm silica spheres after surface modification with initiator moieties and ATRP polymerization of acrylamide for 43 h.

brush swelling in aqueous solution (as measured by DLS) in contrast to its dry state (as measured by SEM). Despite this difference, the resulting polymer brush thicknesses, Δr , determined using both techniques are in good agreement. As shown in Figure 4, the polymer brush thickness increases logarithmically with time, flattens after ca. 12 h, and reaches 15.5 nm after 43 h of polymerization. The relatively slow polymerization rate is suitable for the precise control of polymer brush thickness. For the opal formed from 205 nm silica spheres with a pore size of 16 nm⁵⁷ (the distance from the pore center to the nearest silica sphere surface, Figure 1), it is expected that an almost complete blockage of the pores would be achieved after 12 h of polymerization, assuming a similar polymerization rate and uniform surface coverage.

Surface Polymerization Inside the Opal Film. To determine if the colloidal crystal lattice would remain unperturbed by surface polymerization, we performed ATRP of acrylamide on 7- μm -thick opal films assembled on glass slides using a 1.5 wt % solution of 205 nm silica spheres. The surfaces of the silica spheres were modified with the initiator moieties (Scheme 1), and the polymerization of acrylamide was performed for 43 h. The image of the resulting hybrid opal/poly(acrylamide) film is shown in Figure 5. It is clear that the opal lattice remained intact, although it appears that spheres are “sintered” together (Figure 5, inset) as a result of the polymer brush formation. It is also apparent from Figure 5 that no thick polymeric film is formed over the opal and that opal nanopores are still present. We observed that after polymer modification opal films became more mechanically robust (i.e., they appeared to be “glued” to the electrode surface and would not crack upon impact) compared

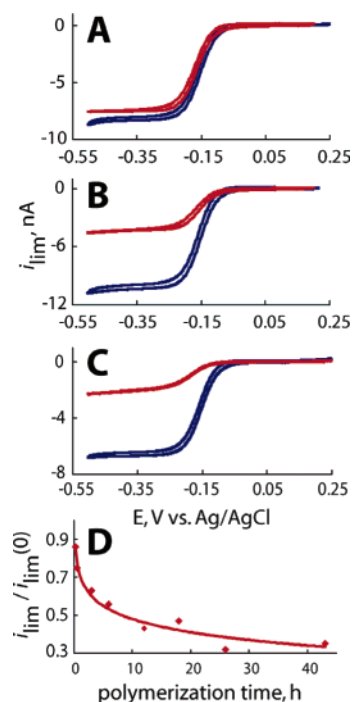


Figure 6. Representative voltammetric responses of opal film Pt electrodes before (blue) and after (red) polymerization for (A) 15 min, (B) 12 h, and (C) 26 h. (D) Plot of relative limiting current as a function of polymerization time.

Table 3. Relative Limiting Current of Opal Film Pt Electrodes as a Function of Polymerization Time and Geometrical Characteristics of Resulting Polymer-Modified Opal Nanopores

polymerization time, h	$i_{\text{lim}}/i_{\text{lim}}(0)$	ϵ	Δr , nm	pore size, nm
0	1.00	0.260	0.0	16.0
0.25	0.86	0.224	1.7	14.3
0.5	0.75	0.195	3.0	13.0
3	0.63	0.164	4.6	11.4
6	0.56	0.146	5.5	10.5
12	0.43	0.122	6.6	9.4
18	0.47	0.112	7.1	8.9
26	0.32	0.083	8.5	7.5
43	0.35	0.091	8.2	7.8

to somewhat brittle unmodified opals, which is a promising property for future applications.

Next, we assembled the opal film on the surface of eight Pt microelectrodes shrouded in glass (Figure 3), modified the opal surfaces with initiator moieties, and polymerized acrylamide on the electrodes while removing them from solution after different periods of time. We then measured the limiting current of Ru-(NH₃)₆³⁺ using these polymer-modified electrodes and compared the current to that before the polymerization. Typical cyclic voltammograms for polymer-modified opal electrodes are shown in Figure 6A–C, and the data are summarized in Table 3. The limiting current calculated for the opal film Pt electrodes using eqs 1 and 2 is in excellent agreement with the measured limiting currents, confirming that point defects visible in the SEM image do not penetrate the entire thickness of the opal film. The relative limiting current measured for the electrodes decreases logarithmically as a function of polymerization time (Figure 6D). We were able to reproduce this result several times. The smooth change in i_{lim} suggests that a uniform polymer brush is being formed inside the nanopores. To confirm that the limiting current is affected only by the polymer formed inside the nanopores, a Pt microelectrode shrouded in glass *without the opal film* was modified with initiator moieties, and acrylamide was polymerized

(56) Jal, P. K.; Patel, S.; Mishra, B. K. *Talanta* **2004**, *62*, 1005–1028 and references therein.

(57) See Supporting Information.

on its surface for 43 h. No decrease in limiting current was observed for this electrode.

The limiting current is proportional to the molecular flux through the opal, J_{opal} ,⁵⁸

$$i_{\text{lim}} = nFAJ_{\text{opal}} \quad (1)$$

where n is the number of electrons, F is the Faraday constant, and A is the electrode area. The molecular flux J_{opal} (mol/cm²·s) through the unmodified opal is described by the following equation⁵⁹

$$J_{\text{opal}} = \frac{\Delta C}{L} \frac{\epsilon_o}{\tau} D_{\text{sol}} \quad (2)$$

where ΔC is the concentration gradient across the opal, L is the thickness of the opal, and D_{sol} is the diffusion coefficient in solution. The void fraction ϵ_o (0.26) and tortuosity τ (ca. 3.0) of an unmodified opal are its intrinsic properties and are independent of the size of silica spheres used to prepare the opal.⁶⁰

Thus, for a given electrode and unchanged measurement conditions, i_{lim} is proportional to the void fraction ϵ' of the polymer-modified opal, and the relative limiting current can be used to calculate ϵ' . Using straightforward geometrical considerations,⁵⁷ we can express the void fraction ϵ' in terms of the silica sphere radius r_o (102.5 nm in our experiments) and polymer-modified sphere radius r_1 as

$$\epsilon' = 1 - \frac{\pi \left(3r_1^2 r_o - \frac{4}{3} r_1^3 - r_o^3 \right)}{2\sqrt{2} r_o^3} \quad (3)$$

The polymer brush thickness $\Delta r = r_1 - r_o$ can be then calculated using this equation and measured values of ϵ' . The results of these calculations are shown in Table 3. The polymer brush

(58) Bard, A. J.; Faulkner, L. R. *Electrochemical Methods: Fundamentals and Applications*, 2nd ed.; Wiley: New York, 2001.

(59) Cussler, E. L. *Diffusion: Mass Transfer in Fluid Systems*, 2nd ed.; Cambridge University Press: New York, 1997.

(60) Newton, M. R.; Morey, K. A.; Zhang, Y.; Snow, R. J.; Diwekar, M.; Shi, J.; White, H. S. *Nano Lett.* **2004**, *4*, 875–880.

thickness increases logarithmically with polymerization time (Figure 4) in a manner similar to that observed for polymerization on silica spheres in solution and reaches 8.5 nm after 26 h. Nanopore size (the distance from the center of the pore to the nearest silica sphere surface) decreases from its initial value of 16 nm for unmodified opal to 7.5 nm for the polymer-modified nanopores after 26 h of polymerization (Table 3). The polymerization rate inside the opal is ca. 2 times slower than that in colloidal solution, which likely results from the slower diffusion of the monomer to the silica sphere surface inside the nanopores. It is important to note that the polymer thickness calculated using eq 3 is based on the assumption that the polymer behaves as an impermeable solid. If the diffusion coefficient through the polymer brush for redox species used in this study is nonzero, then diffusion through the polymer brush cannot be ignored, and the actual polymer brush thickness would be somewhat larger compared to that given in Table 3.

Conclusions

We demonstrated for the first time that surface-initiated ATRP of acrylamide can be conducted inside opal nanopores. It does not perturb the opal lattice and leads to uniform polymeric brushes inside the opal nanopores. The size of the resulting polymer-modified nanopores can be controlled by the polymerization time. Nanopores with sizes from 16 to 7.5 nm (the distance from the center of the pore to the nearest silica sphere surface) have been prepared in this manner. We are presently studying the modification of opal nanopores with stimuli-responsive polymers.

Acknowledgment. I. Z. is grateful to the Camille and Henry Dreyfus Foundation for a New Faculty Award. We thank Professor Chuck White and Ms. Jeramie Jergins (Chemistry Department, University of Utah) for assistance with TGA measurements, Professor Jakub Nalaskowski (Metallurgical Engineering Department, University of Utah) for help with DLS measurements, and Professor Christopher Hacon (Mathematics Department, University of Utah) for help with geometrical derivations.

Supporting Information Available: Details of the opal nanopore geometry and derivation of eq 3. This material is available free of charge via the Internet at <http://pubs.acs.org>.

LA061170D